TOXICOLOGICAL SCIENCES **113(1)**, 254–266 (2010)
doi:10.1093/toxsci/kfp213
Advance Access publication October 7, 2009

The Role of Hypoxia in 2-Butoxyethanol–Induced Hemangiosarcoma

Daphna Laifenfeld,* Annalyn Gilchrist,* David Drubin,* Milena Jorge,* Sean F. Eddy,* Brian P. Frushour,* Bill Ladd,* Leslie A. Obert,† Mark M. Gosink,† Jon C. Cook,† Kay Criswell,† Christopher J. Somps,† Petra Koza-Taylor,† Keith O. Elliston,* and Michael P. Lawton†,[1]

*Genstruct, Inc., Cambridge, Massachusetts 02140; and †Pfizer Global Research and Development, Groton, Connecticut 06340

[1] To whom correspondence should be addressed at Pfizer Global Research and Development, Eastern Point Road, MS8274-1234, Groton, CT 06340. E-mail: michael.lawton@pfizer.com.

Received July 6, 2009; accepted September 4, 2009

To understand the molecular mechanisms underlying compound-induced hemangiosarcomas in mice, and therefore, their human relevance, a systems biology approach was undertaken using transcriptomics and Causal Network Modeling from mice treated with 2-butoxyethanol (2-BE). 2-BE is a hemolytic agent that induces hemangiosarcomas in mice. We hypothesized that the hemolysis induced by 2-BE would result in local tissue hypoxia, a well-documented trigger for endothelial cell proliferation leading to hemangiosarcoma. Gene expression data from bone marrow (BM), liver, and spleen of mice exposed to a single dose (4 h) or seven daily doses of 2-BE were used to develop a mechanistic model of hemangiosarcoma. The resulting mechanistic model confirms previous work proposing that 2-BE induces macrophage activation and inflammation in the liver. In addition, the model supports local tissue hypoxia in the liver and spleen, coupled with increased erythropoeitin signaling and erythropoiesis in the spleen and BM, and suppression of mechanisms that contribute to genomic stability, events that could be contributing factors to hemangiosarcoma formation. Finally, an immunohistochemistry method (Hypoxyprobe) demonstrated that tissue hypoxia was present in the spleen and BM. Together, the results of this study identify molecular mechanisms that initiate hemangiosarcoma, a key step in understanding safety concerns that can impact drug decision processes, and identified hypoxia as a possible contributing factor for 2-BE–induced hemangiosarcoma in mice.

Key Words: **hemangiosarcoma; hypoxia; angiogenesis; endothelial cells; endothelial precursor cells; mechanism of action; human relevance; 2-butoxyethanol.**

Hemangiosarcomas are endothelial cell (EC)–derived tumors that are comprised of poorly differentiated, proliferating ECs (Mendenhall *et al*., 2006). These tumors form spontaneously and in response to many different compounds in mice (NTP, 1993; Wagner and Risau, 1994) but are rare in humans (Mendenhall *et al*., 2006). Compounds that induce hemangiosarcomas in mice have a wide range of biological activity and include industrial, natural, and pharmaceutical compounds (Chan, 1993; Cohen *et al*., 2009; El-Hage, 2004; NTP, 1989, 1993, 1997, 2000, 2004). The discovery that a potentially therapeutic compound induces hemangiosarcomas in mice may limit it from further development or broader applications. A detailed understanding of the molecular mechanisms underlying the formation of these tumors in mice may therefore lead to a better assessment of the risk to humans from exposure to such compounds.

Many of the compounds that induce hemangiosarcomas in mice, including 2-butoxyethanol (2-BE), *p*-chloroaniline (Nyska *et al*., 2004), *p*-nitroaniline (Nyska *et al*., 2004), 2-biphenylamine (Abdo *et al*., 1982), and phenylhydrazine (Goldberg and Stern, 1977; Toth *et al*., 1978), are hemolytic in nature. 2-Butoxyethanol, a chemical solvent that has been shown to induce hemangiosarcomas mainly in livers of male mice (Nyska *et al*., 2004), with some occurrence in the bone marrow (BM) and spleen after inhalation exposure (NTP, 2000), has been used as a model hemangiosarcoma-inducing agent to further understand the mode of action of tumor formation (Cohen *et al*., 2009; Corthals *et al*., 2006; Klaunig and Kamendulis, 2005; Park *et al*., 2002a,b; Siesky *et al*., 2002). The results of this work support a nongenotoxic mode of action that centers on macrophage activation due to iron accumulation resulting from the hemolytic effect of the compound (Elliot and Ashby, 1997; Klaunig and Kamendulis, 2005; Park *et al*. 2002a,b). Macrophage activation, in turn, is proposed to promote EC proliferation and DNA damage via the production of reactive oxygen species and cytokines that stimulate EC proliferation (Klaunig and Kamendulis, 2005; Park *et al*., 2002a; Siesky *et al*., 2002).

In addition to the proposed EC proliferation caused by macrophage activation, it is possible that localized or systemic hypoxia associated with hemolysis can also contribute to EC proliferation. Hypoxia and activation of the hypoxia-inducible factor, Hif1, have been shown to promote EC proliferation (Otrock *et al*., 2009; Yamakawa *et al*., 2003), which, if sustained, can result in cellular transformation as a result of errors during DNA replication that are not repaired. There is also growing evidence that hypoxia can drive and maintain genetic instability leading to increased rates of mutagenesis,

thus contributing to a "mutator" phenotype (Bristow and Hill, 2008). Taken together, it is plausible that the significant hemolysis caused by 2-BE results in local tissue hypoxia, which may in turn contribute to EC proliferation leading to the induction of hemangiosarcoma in mice.

To investigate whether tissue hypoxia plays a role in the induction of hemangiosarcoma by 2-BE, a systems biology approach called Causal Network Modeling (CNM) was undertaken, in which transcriptomic signatures of 2-BE in liver, spleen, and BM from mice were used to elucidate the molecular pathways that contribute to hemangiosarcoma formation. CNM is a systematic computational analysis that identifies upstream changes in gene regulation that can serve as explanations for observed changes in gene expression. This approach has been successfully used to identify molecular mechanisms involved in Sirtuin 1-induced keratinocyte differentiation (Blander *et al*., 2009) and the development of type II diabetes (Pollard *et al*., 2005).

The present study is the first to identify molecular mechanisms underlying hematopoietic events that contribute to hemangiosarcoma formation in mice treated with 2-BE. The results confirm previously identified mechanisms associated with hemangiosarcoma formation, including inflammation and macrophage activation. Moreover, novel mechanisms as contributing factors to hemangiosarcoma formation were also identified, including hypoxia, leading to increased Erythropoeitin (Epo) signaling and erythropoiesis in the spleen and BM, as well as suppression of mechanisms that contribute to genomic stability. These results also support the recruitment of proliferating endothelial progenitor cells (EPCs) in the BM to sites of inflammation in the liver as a mechanism of hemangiosarcoma formation. The proposed mode of action is consistent with that recently reported by Cohen *et al*. (2009) and may serve as a general framework for other hemolytic compounds that also cause hemangiosarcomas in mice.

MATERIALS AND METHODS

Animal studies (general). In all, 9- to 11-week-old B6C3F1 male mice, weighing about 30 g (Charles River Breeding Laboratories, Raleigh, NC) were acclimatized, randomized into treatment groups, and housed individually in each study. Room environmental conditions had design specifications as follows: minimum of 12 air changes per hour with air filtered through 90–95% efficiency filters and then through high efficiency particulate air filters, relative humidity of 50 ± 10%, temperature of 70°F ± 5°F, and a 12-h light/dark cycle. Certified Rodent Diet 5002 (PMI Feeds, Inc., St. Louis, MO) and municipal drinking water, further purified by reverse osmosis, were provided *ad libitum*. The animal care and experimental procedures of these studies were conducted in compliance with the U.S. Animal Welfare Act and were performed in accordance with the standards of the Institute of Laboratory Animal Resources Guide (1996). The Association for Assessment and Accreditation of Laboratory Animal Care International has accredited the Pfizer facility in which the studies were conducted.

2-BE studies. Mice were administered either 900 mg/kg 2-BE (Sigma-Aldrich, St Louis, MO) in deionized water or deionized water alone by oral gavage daily for 7 days (10 animals per treatment group). Each dose group was further divided into two arms, one ($n = 5$) for Hypoxyprobe (NPI, Burlington, MA) immunohistochemical (IHC) staining and the other ($n = 5$) for RNA isolation and transcriptional profiling. Hypoxyprobe was injected i.p. 2.5 h prior to sacrifice. Additional treatment groups (four animals per group) received only a single dose of 2-BE (900 mg/kg) or deionized water by oral gavage and were sacrificed 4 h after dosing for gene expression analysis. Red blood cell (RBC) counts and hemoglobin (Hgb) were determined using an Advia 120 hematology analyzer (Siemens, Tarrytown, NY) to verify hemolytic effects. All animals were anesthetized with ketamine and sacrificed by cervical dislocation. BM (left femur), liver, and spleen were collected in 10% neutral buffered formalin (NBF) and processed using routine methods for microscopic evaluation. The dose chosen for the 2-BE studies (900 mg/kg) was based on Siesky *et al*. (2002), where treatment of mice with 900 mg/kg 2-BE for 7 days produced a significant decrease in hematocrit, and on Park *et al*. (2002b), where 900 mg/kg 2-BE for 7 days also produced oxidative stress in the liver.

Hypoxia studies. Mice were subjected to either whole-body hypoxia or normoxia. Unrestrained mice were treated in a plethysmography chamber (PLY 3211; Buxco Research Systems, Wilmington, NC) connected to a Bias Flow Regulator (PLY1040; Buxco Research Systems), which provided normobaric airflow of 1.0–1.5 ml/min. Mice ($n = 4$) were exposed to hypoxia that followed a course of 8% O_2 pretreatment for 30 or 60 min followed by a 60- to 90-min 6% O_2 treatment. Control mice ($n = 4$) were exposed to normal air in the plethysmography chambers for an equal duration. Mice were sacrificed by cervical dislocation immediately following hypoxia treatment. Tissues were evaluated for gene expression or Hypoxyprobe immunohistochemistry.

Hypoxyprobe IHC staining. Hypoxyprobe (pimonidazole HCl) uses an IHC method for the detection of local tissue hypoxia (http://www.hypoxyprobe.com). In a low oxygen environment, the pimonidazole is reductively activated and binds to cysteine residues and thiols forming protein adducts in hypoxic cells that are detected using standard IHC methods. The reagent has been used to detect local tissue hypoxia in liver (Arteel *et al*., 1996). Liver, spleen, and BM (from femurs) from mice injected with Hypoxyprobe were extracted and immediately placed in ice-cold 10% NBF for 24 h. BM samples were subsequently placed in ImmunoCAL (Decal Chemical, Tallman, NY) for an additional 24 h. All tissues were processed and embedded in paraffin blocks according to standard procedures. Tissue sections were cut at 5 μm and placed on glass slides. Citrate antigen retrieval was done using high heat and pressure (Chemicon, Temecula, CA) followed by peroxidase block (Sigma-Aldrich) and protein block (Dako, Carpinteria, CA). IHC staining was performed at room temperature on an automated Dako Autostainer (Dako). The Hypoxyprobe reagent was run at a dilution of 1/500 for 60 min, detected using Dako Envision+ Rabbit HRP Polymer for 30 min at room temperature, and then visualized with Dako Liquid DAB+. Slides were counterstained with Mayer's hematoxylin and cover slipped. Negative controls for the study included a rabbit isotype control antibody (Dako) incubated for 60 min. In addition, tissue samples from animals not treated with pimonidazole were stained with the same protocol to show the absence of nonspecific anti-Hypoxyprobe antibody staining. All images were captured at ×20 using a Hammamatsu NanoZoomer (Olympus, Center Valley, PA) slide scanner and stored in a Bacus image format. Definiens (Munich, Germany) image analysis software was used to calculate the stain ratio (stain area/tissue area). See Supplementary Materials for more details on image quantification.

RNA isolation and transcriptional profiling. A portion of the left lateral liver lobe and a half cross-section of spleen were rapidly dissected from mice and flash-frozen in liquid nitrogen. The BM cells were collected via a BM flush utilizing 700 μl Paxgene BM buffer (Qiagen, Inc., Valencia, CA) from the right humerus and frozen at −80°C. Total RNA was extracted from a minimum of four mice per treatment group, along with corresponding vehicle controls. The frozen liver and spleen were crushed, and 50–100 mg of the crushed tissue was used to prepare total RNA by extracting in Trizol (Invitrogen, Carlsbad, CA) followed by purification on a Qiagen RNeasy Mini column as recommended by the manufacturer (Qiagen, Inc.). Total RNA was isolated from the BM in Paxgene buffer as recommended by the manufacturer (Qiagen, Inc.). The

quantity and purity of the RNA were determined by absorbance at 260 and 260 nm/280 nm absorbance ratio, respectively. Each of the total RNA preparations was individually assessed for RNA quality based on the 28S/18S ratio measured on an Agilent 2100 Bioanalyzer system using the RNA 6000 Nano LabChip Kit. complementary DNA (cDNA) was synthesized using 2 μg of high-quality total RNA. SuperScript II (Invitrogen) was used to reverse transcribe the mRNA in the presence of a T7-containing oligo-dT24 primer followed by second-strand synthesis as recommended by Affymetrix (Santa Clara, CA) cDNA was purified using RNAClean magnetic beads (Agencourt Bioscience Corp., Beverly, MA) and used as a template for *in vitro* transcription using the GeneChip One-Cycle Labeling Kit from Affymetrix. Complmentary RNA (cRNA) was purified using magnetic beads from Agencourt Bioscience Corp., and the quantity and purity of the cRNA were determined by absorbance at 260 and 260 nm/280 nm absorbance ratio, respectively. The quality of the cRNA was evaluated by assessing the size distribution of the cRNA using a 1.25% 3-(N-morpholino)propanesulfonic acid gel.

The labeled cRNA was fragmented as recommended by Affymetrix and 10 μg was added to a hybridization cocktail prior to loading onto individual Mouse 430 2.0 GeneChip microarrays. The microarrays were hybridized at 45°C for 16–24 h and washed and stained on an Affymetrix FS450 fluidics station according to the manufacturer recommendations. The microarrays were scanned on a GeneChip Scanner 3000.

Array data quality was evaluated using a proprietary high-throughput application that assesses the data against multiple objective standards including 5′/3′ glyceraldehyde 3-phosphate dehydrogenase ratio, signal/noise ratio, and background as well as other additional metrics (e.g., outlier, vertical variance) and a visual inspection of the chip image for surface defects. All samples passed these data quality assessments.

Determination of significant RNA expression changes. RNA expression data were analyzed using the "affy" and "limma" packages of the Bioconductor suite of microarray analysis tools available for the R statistical environment (Gentleman, 2005; Gentleman *et al*., 2004; Irizarry *et al*., 2003; R Development Core Team, 2007). Robust microarray analysis background correction and quantile normalization were used to generate microarray expression values. Prior to analysis of changing genes, data were visualized using principal components analysis and hierarchical clustering to identify outlier samples. Three samples (one control each in 2-BE 7-day liver, 2-BE 4-h liver, and hypoxia BM) were judged to be sufficiently different from others in their treatment cohorts that they were not used for further analysis. An overall linear model was fit to the data for all sample groups, and specific contrasts of interest were evaluated to generate raw p values for each probe set on the expression array (Smyth, 2004). The Benjamini-Hochberg false discovery rate method was then used to correct for multiple testing effects. Probe sets were considered to have changed qualitatively in a specific comparison if an adjusted p value of 0.05 was obtained, their average expression intensity was above 150 in either treatment group, and they had an absolute fold change greater than 1.3. Genes represented by multiple probe sets were considered to have changed if at least one probe set was observed to change. Gene expression changes that met these criteria were called statistically significant RNA expression changes and have the directional qualities of "up" or "down" (i.e., they can be upregulated or downregulated in response to treatment).

Knowledgebase and mouse knowledge assembly model. The substrate for analysis of statistically significant RNA gene expression changes in response to a given treatment is the mouse knowledge assembly Model, which is derived from the global Genstruct Knowledgebase. This knowledge base is a collection of biological concepts and entities and their causal relationships that is derived from peer-reviewed scientific literature as well as public and proprietary databases. The Mouse Knowledge Assembly Model is the set of mouse-specific causal assertions that has been augmented with orthologous causal assertions derived from either rat or human sources and is competent for causal modeling. An example causal assertion would be increased transcriptional activity of nuclear factor kappa-light-chain-enhancer of activated B cells (NF-κB) complex causing an increase in the gene expression of the insulin receptor substrate 1 (Irs1) (Ruan *et al*., 2002). Each causal assertion has a specific scientific citation, and the assembled collection of these causal assertions is referred to as the Mouse Knowledge Assembly Model in this article.

The CNM. In the case of RNA expression data, CNM interrogates the Mouse Knowledge Assembly Model to identify upstream controllers for the statistically significant gene expression changes observed in the experiment. These upstream controllers are called hypotheses as they are statistically significant potential explanations of the gene expression changes. Hypothesis generation is performed automatically by a computer program that utilizes the Mouse Knowledge Assembly Model to identify hypotheses that explain the input gene expression changes, prioritized by multiple statistical criteria. Each hypothesis is scored according to two probabilistic scoring metrics, richness and concordance, that examine distinct aspects of the probability of a hypothetical cause explaining a given number of statistically significant gene expression changes. Richness is the probability that the number of observed gene expression changes connected to a given hypothesis could have occurred by chance alone. Concordance is the probability that the number of observed gene expression changes that match the directionality of the hypothesis (e.g., increased or decreased kinase activity for a kinase, increased or decreased transcriptional activity for a transcription factor, etc.) could have occurred by chance alone. For each hypothesis "Score" is the number of gene expression changes that support the hypothesis in its statistically significant direction, and "Contra" is the number of gene expression changes that support an opposite direction for the hypothesis. A hypothesis was considered to be statistically (although not necessarily biologically) significant if it met richness and concordance probability cutoffs of 0.05 and marginally significant if it met richness and concordance probability cutoffs of 0.1. These hypotheses are further investigated and prioritized by evaluation of their biological relevance to the experimental context, whether they are causally linked to phenotypes and processes relevant to hemangiosarcoma formation in the literature and if they are causally downstream of the experimental treatments. The models for each organ in response to 2-BE were merged to create the overall mechanistic model for hemangiosarcoma formation.

RESULTS

Confirmation of Hemolysis Induced by 2-BE

Hematology. As shown in Table 1, RBC and Hgb were decreased 23% at 4 h. After 7 days of treatment, RBC was decreased 23% and Hgb was decreased 19%. Reticulocyte counts were unchanged from untreated controls at 4 h but increased by 6.1-fold at 7 days. These results confirm that active hemolysis was present within 4 h of 2-BE administration and that RBC and Hgb remained significantly decreased compared to untreated controls regardless of enhanced erythropoietic activity (i.e., increased reticulocyte counts) after 7 days of treatment.

Histopathology. After 7 days of 2-BE treatment, microscopic findings included increased splenic extramedullary hematopoiesis (EMH) and decreased BM myeloid:erythroid (M:E) ratio. Increased splenic EMH was characterized by increased numbers of hematopoietic precursors in the medullary red pulp with a predominance of erythroid lineage cells. Similarly, the decreased M:E ratio observed in the BM was characterized by increased numbers of erythroid lineage cells (i.e., erythroid hyperplasia) compared to myeloid precursors. These findings are consistent with a compensatory mechanism to replenish the RBC pool following 2-BE–induced hemolysis. Histopathology was not measured at the 4-h time point.

TABLE 1
RBC Counts, Hgb Concentrations, and Reticulocyte Counts in Mice following 2-BE Administration for 4 h or 7 Days[a]

Parameter	Untreated control (4 h, $n = 10$)	2-BE (900 mg/kg) (4 h, $n = 10$)	Untreated control (7 days, $n = 5$)	2-BE (900 mg/kg) (7 days, $n = 4$)
RBC (10^6/μl)	9.63 ± 0.43	7.38 ± 0.73[b]	9.71 ± 0.33	7.47 ± 0.40[b]
Hgb (g/dl)	14.6 ± 0.87	11.2 ± 0.69[b]	15.1 ± 0.50	12.2 ± 0.77[b]
Reticulocyte count (10^3/μl)	248.3 ± 43.7	299.6 ± 86.9	171.7 ± 28.0	1045.5 ± 245.2[b]

[a]Four-hour hematology data were collected from earlier 2-BE studies and reported here for reference.
[b]Group mean significantly different from control at level $p = 0.01$. Arithmetic means and SDs were calculated, and treatment comparisons were performed using Student's *t*-test applied at the two-tailed 1% significance level.

Overview of CNM Results

To build a model of 2-BE–induced hemangiosarcoma, CNM was used to identify statistically significant explanations or hypotheses for the observed gene expression changes induced by 4 h and 7 days 2-BE treatment in the BM, spleen, and liver of B6C3F1 mice (Table 2); 7-day treatment was used to identify molecular mechanisms that can lead to hemangiosarcoma formation, while the 4-h treatment served to identify potential initiating events for these mechanisms. The model was then compared to the transcriptomic fingerprint generated in mice treated directly with hypoxia (2 h, 6–8% O_2). Table 2 lists the number of gene expression changes and hypotheses that explain these changes for all treatments and tissue combinations.

Confirmation of Previous Findings that 2-BE Induces Macrophage Activation and Inflammation in the Liver

Analysis of mice treated with 2-BE for 4 h identified increased transcriptional responses to inflammation and oxidative stress in spleen and liver (Supplementary Figs. 1A–D). At the 7-day time point, CNM also predicted an increase in inflammation in the liver (Fig. 1), which, like the results at 4 h, is consistent with publications from Klaunig and colleagues (Corthals *et al.*, 2006; Klaunig and Kamendulis, 2005). An

TABLE 2
Overview of the Number of RNA Expression Changes and Hypotheses Identified in Each Tissue in Response to Each Treatment[a]

Tissue	Treatment	Gene expression changes	Biologically relevant hypotheses
BM	2-BE 4 h	0	ND
	2 BE 7 days	1236	72
	Hypoxia	511	74
Spleen	2-BE 4 h	465	144
	2 BE 7 days	2115	ND
	Hypoxia	1442	74
Liver	2-BE 4 h	200	71
	2 BE 7 days	155	26
	Hypoxia	781	81

Note. ND, not determined (see the ''Results''section for explanations).
[a]The process used to identify the gene expression changes meeting statistical significance and the number of hypotheses identified by CNM for each treatment and network are outlined in the ''Materials and Methods'' section. More details about the individual hypotheses can be found in Supplementary Table 1.

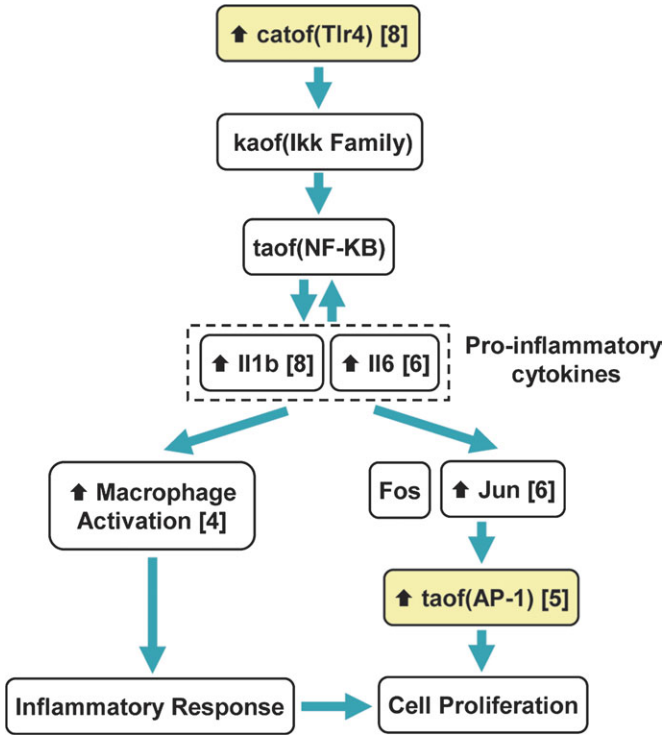

FIG. 1. Seven-day 2-BE treatment induces inflammation in the liver. CNM based on gene expression changes supports a proinflammatory response in which Tlr4 induces an increase in NF-κB transcriptional activation, leading to cytokine production and macrophage activation. Notation and color guide: Numbers in brackets indicate the number of gene expression changes supporting a given hypothesis; catof(X) is catalytic activity of X; kaof(X) is kinase activity of X; taof(X) is transcriptional activity of X; yellow boxes are statistically significant predicted increases in the activity or abundance of the protein indicated in a given hypothesis with a concordance *p* value less than 0.05; white boxes with an arrow are significant hypotheses with a concordance *p* value between 0.05 and 0.1; white boxes without an arrow are not significant hypotheses and are presented for clarity; connecting lines with arrowheads indicate a causal activation. Genes that support the hypotheses listed in this figure can be found in Supplementary Table 2.

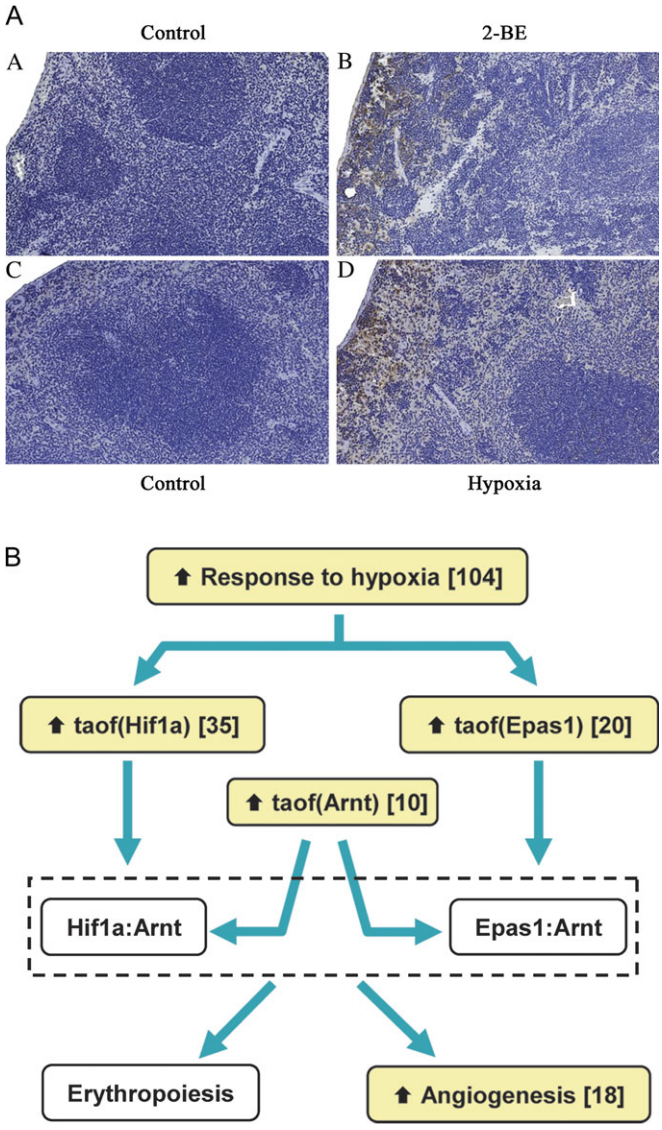

FIG. 2. 2-BE treatment leads to hypoxia in the spleen. (A) IHC detection of hypoxia by Hypoxyprobe after seven consecutive doses of 2-BE and after acute hypoxia (6–8% O_2, 1.5–2.5 h). Representative images of tissue sections from animals treated with 2-BE (A, control; B, treated) or hypoxia (C, control; D, treated) are shown. (B) Molecular response to hypoxia in the spleen 4 h following a single dose of 2-BE based on CNM. For notation and color guide, see Figure 1 legend. Genes that support the hypotheses listed in Figure 2B can be found in Supplementary Table 3.

increase in inflammation was supported by increased catalytic activity of Tlr4, evidenced by eight gene expression changes (Supplementary Table 2). Increases in the levels of the proinflammatory cytokines Il1b and Il6 in the liver were also supported by eight and six gene expression changes, respectively (Fig. 1). Increases in cytokines are consistent with macrophage activation. As illustrated in Figure 1, Tlr4 promotes inflammation by inducing the transcriptional activity of NF-κB, which leads to proinflammatory cytokine production (O'Neill and Bowie, 2007) that in turn activates AP-1

TABLE 3
Summary of Hypoxyprobe Immunohistochemistry Quantitation Data from BM, Spleen, and Liver of Mice Treated with 2-BE (900 mg/kg) or Hypoxia (6–8% O_2, 1.5–2.5 h)[a]

Tissue	Treatment	Fold change (over control)[b]
BM	2-BE 7 days	↑ 2.41 ($p = 0.044$)
	Hypoxia	↑ 6.89 ($p = 0.015$)
Spleen	2-BE 7 days	↑ 19.00 ($p = 0.028$)
	Hypoxia	↑ 5.60 ($p = 0.094$)
Liver	2-BE 7 days	No change
	Hypoxia	↑ 3.05 ($p = 0.005$)

[a]Experimental details for the hypoxia treatment can be found in the Supplementary Materials.
[b]A two-sample *t*-test was used to compare the treated and control groups. A Levene's test was applied to determine if the *t*-test would be performed under unequal or equal variance conditions.

signaling, which has been shown to stimulate cell proliferation (Ballermann *et al.*, 1998).

Support for Hypoxia as an Initiating Event for 2-BE–Induced Hemangiosarcoma

In addition to confirming previously reported increases in inflammation and oxidative stress, CNM also identified hypoxia as a molecular response in spleen and liver in mice treated with 2-BE for 4 h and in spleen and BM in mice treated with 2-BE for 7 days. This response was then compared to the transcriptomic fingerprint generated in mice treated directly with reduced oxygen as a positive control for hypoxia. In addition, Hypoxyprobe immunohistochemistry was used to quantitate hypoxia in the same organs following these treatments. The sections that follow describe the support for hypoxia as an initiating event. See Supplementary Materials for a more detailed overview of the CNM and IHC results following treatment with hypoxia. Briefly, CNM provided evidence for oxidative stress and a transcriptional response to hypoxia in liver, spleen, and BM of mice following exposure to 6–8% O_2 for 1.5–2.5 h.

2-BE 4-h treatment leads to hypoxia in spleen and liver. A transcriptional response to hypoxia was supported in response to the 2-BE 4-h treatment in both the spleen and liver (Fig. 2B and Supplementary Figs. 1C and D). Detection of a transcriptional response in the spleen that supports hypoxia after 2-BE 4-h treatment is consistent with the Hypoxyprobe results for this organ after 2-BE 7-days treatment, where a 19-fold increase was observed in IHC staining for hypoxia (Fig. 2A, panel B, Table 3). The transcriptional response in the spleen that supports hypoxia includes the activation of the hypoxia-inducible transcription factors Hif1a, Epas1, and Arnt, supported by 35, 20, and 10 gene expression changes, respectively (Fig. 2B). Similarly, in the liver, CNM identified increased transcriptional responses to hypoxia after 4-h

treatment with 2-BE, which is supported by increases in the activities of Hif1a and Epas1 and evidenced by 15 and 9 gene expression changes, respectively (Supplementary Fig. 2A). 2-BE 4-h treatment in the BM did not yield significant gene expression changes for CNM (Table 2).

2-BE 7-day treatment leads to hypoxia in the spleen and BM. In the BM, CNM identified inhibition of Hif1a transcriptional activity as well as a decrease in a general transcriptional response to hypoxia after 2-BE 7-day treatment, supported by 48 and 157 gene expression changes, respectively (Supplementary Fig. 3). These molecular responses are consistent with a response in mice to prolonged hypoxia that leads to Hif1a desensitization (Ginouves *et al.*, 2008; Stroka *et al.*, 2001). Hypoxyprobe was used to determine whether 2-BE treatment for 7 days leads to immnohistochemically detectable hypoxia in the BM, spleen, and liver. Increased hypoxia was detected by Hypoxyprobe in both the spleen (Fig. 2A, panels A and B) and the BM after 2-BE 7-day treatment (Table 3). CNM was not performed on the spleen 2-BE 7-day treated data set due to the robust induction of erythropoiesis in this organ. In the liver, CNM and Hypoxyprobe measurements after 2-BE 7-day treatment did not support hypoxia or a hypoxic response (data not shown).

Hypoxia Can Lead to Epo-Induced Cell Proliferation and Differentiation following 2-BE Treatment

2-BE 7-day treatment increases epo-induced erythrocyte differentiation and proliferation and EPC/EC proliferation in the BM. CNM supports an induction of Epo signaling in the BM of B6C3F1 mice in response to 2-BE 7-day treatment, consistent with the stimulatory effect of hemolysis on erythropoiesis. An increase in Epo levels was supported in the BM by 58 gene expression changes (Supplementary Table 4). Epo triggers differentiation and proliferation of erythroid cells via kirsten rat sarcoma viral oncogene homolog (Kras) and the phosphatidyl inositol 3-kinase (PI3K)/protein kinase B (Akt) pathway (Bouscary *et al.*, 2003; Zhang and Lodish, 2005), resulting in phosphorylation and activation of the erythroid differentiation transcription factor Gata1 (Jelkmann, 2004) (Fig. 3). Consistent with this, CNM identified activation of Kras, supported by 37 gene expression changes, as well as activation of the PI3K/Akt pathway (Fig. 3). Activation of the latter pathway was supported via decreased activities of the PI3K/Akt pathway inhibitor, Pten (Chow and Baker, 2006) and Foxo1, which are negatively regulated by Akt (Burgering and Kops, 2002). Decreased Pten and Foxo1 activities were supported by 72 and 36 gene expression changes, respectively. In addition, increased Gata1 activity was supported in the BM by 23 gene expression changes (Fig. 3). CNM also supports increased iron accumulation in the BM via an increase in the transferrin receptor, Tfrc, which is involved in transporting iron into the cell for erythropoiesis. Together, increased Epo, Akt signaling, Gata1 activity, and iron accumulation support increased erythroid differentiation and proliferation in the BM (Fig. 3), an expected response to 2-BE treatment due to its hemolytic effects.

In addition to its role in erythropoiesis, Epo signaling has also been shown to stimulate the differentiation and proliferation of EPCs and ECs via activation of the PI3K/Akt pathway (Bahlmann *et al.*, 2004; Urao *et al.*, 2006). CNM supports increased Epo signaling via activation of the PI3K/Akt pathway following 2-BE treatment (Fig. 3). Since hemangiosarcomas are tumors of endothelial origin, increased Epo signaling and activation of the PI3K/Akt pathway following 2-BE treatment should lead to increased EPC/EC cell proliferation in the BM.

2-BE 7-day treatment increases epo-induced erythrocyte differentiation and proliferation and EPC/EC proliferation in the spleen. The spleen has been reported to be the main site for stress-induced erythropoiesis in mice (Hiroyama *et al.*, 2008), and EMH would be anticipated as a stress response to a hemolytic agent. The induction of Epo in response to 7-day 2-BE treatment confirmed the induction of erythropoiesis in the spleen. Consistent with this, increased expression of multiple markers of nucleated erythrocytes (Chambers *et al.*, 2007) and enzymes involved in synthesizing Hgb (Table 4) (Heinemann *et al.*, 2008), the oxygen-binding component of erythrocytes, were observed in the spleens of mice after 2-BE 7-day treatment. Additionally, increased expression of Tfrc, which is necessary for iron import into the cell for heme synthesis, was also observed (Table 4). Notably, of the gene expression changes observed in the spleen, genes related to erythropoiesis (Chambers *et al.*, 2007; Ding *et al.*, 2004; Peters *et al.*, 1999; Tao *et al.*, 2000; Yi *et al.*, 2006) showed the highest expression changes with 2-BE treatment (Supplementary Table 5), supporting massive erythropoiesis in this organ. The robust induction of erythropoiesis led to an uneven distribution of cell types between control and treated samples, with the treated samples having a much larger proportion of erythrocytes compared to control. This uneven cell type distribution did not allow for a meaningful comparison between treated and control samples, and therefore, CNM was not carried out for this organ. As previously described, Epo signaling in the BM can result not only in erythropoiesis but also in proliferation of EPCs/ECs.

Additional Effects on Cell Proliferation, Differentiation, and Genomic Stability

In addition to the confirmation of previous findings supporting inflammation and macrophage activation, and the complementary evidence of hypoxia, 2-BE was also found to induce several other processes not previously identified but relevant for events that contribute to hemangiosarcomas.

2-BE 7-day treatment induces cell cycle progression in the BM. Multiple mechanisms leading to cell cycle progression were supported in the BM of 2-BE–treated mice at 7 days.

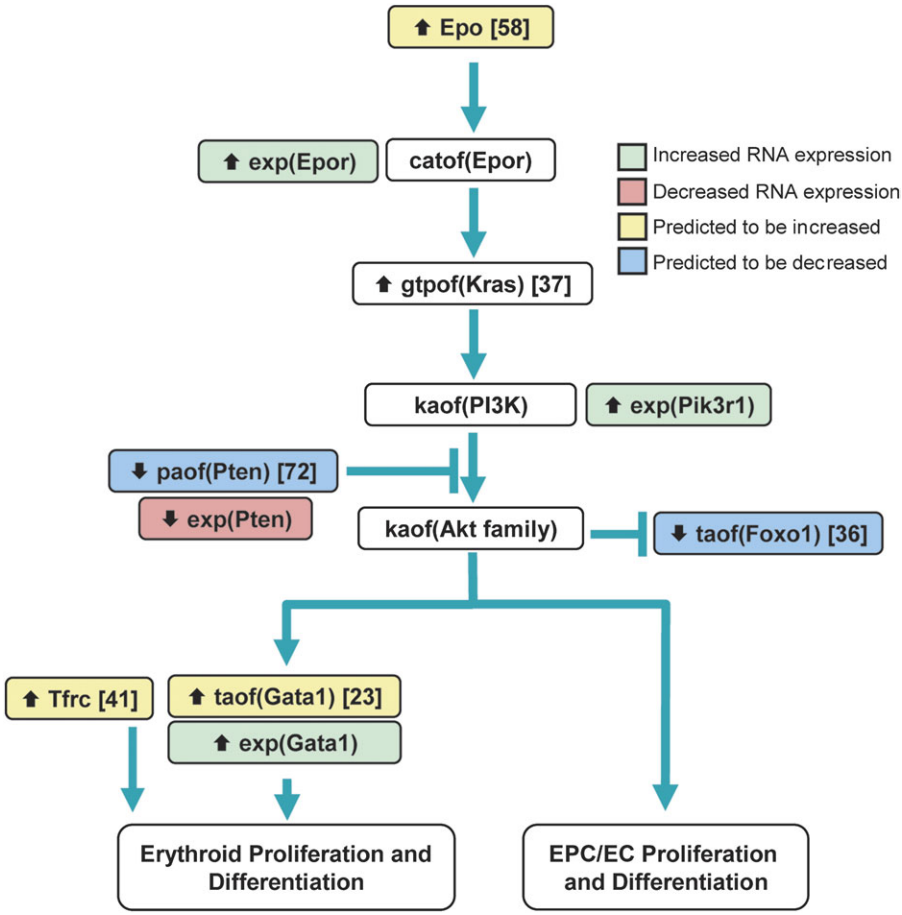

FIG. 3. Seven-day 2-BE treatment leads to erythropoiesis and EC/EPC proliferation in the BM. CNM based on BM gene expression changes predicts increased Epo signaling that leads to erythropoiesis via increased transcriptional activity of Gata1. Notation and color guide: paof(X) is phosphatase activity of X; gtpof(X) is guanosine triphosphate-bound activity of X; exp(X) is expression of X; connecting lines with arrowheads indicate a causal activation; lines with bars indicate causal inhibition; blue boxes are statistically significant predicted decreases in the activity or abundance of the protein indicated in a given hypothesis with a concordance p value less than 0.05; green and red boxes are statistically significant increases or decreases in the expression levels of the indicated mRNA, respectively. For additional notation, see Figure 1. Genes that support the hypotheses listed in this figure can be found in Supplementary Table 4.

These cell cycle mechanisms can be induced by Akt signaling, consistent with the previously mentioned role of the Akt pathway in triggering proliferation of erythrocytes and EPCs/ECs (Bahlmann *et al*., 2004; Urao *et al*., 2006). CNM supports increased protein levels of cell cycle activators, including the cyclin Ccnd1 and the transcription factors Myc, E2f1, and E2f3, supported by 21, 62, 15, and 5 gene expression changes, respectively (Fig. 4). Moreover, decreased cell cycle inhibitors were observed, including decreased levels of Cdkn1a and Cdkn2a, and in the transcriptional activities of Rb1 and E2f4, supported by 21, 13, 26, and 23 gene expression changes, respectively (Fig. 4). Increased expression of Ccne1, a cell cycle activator, was also observed. Together, these factors constitute a robust pathway (Fig. 4), contributing to the increase in proliferation of both erythrocytes and EPCs/ECs in the BM in response to 2-BE 7-day treatment.

2-BE 7-day treatment decreases levels of Bnip3l. CNM supports decreased Bnip3l protein abundance in the BM, based on 49 gene expression changes (Supplementary Table 3). Since Bnip3l is essential for autophagic removal of mitochondria during maturation of erythroid cells (Sandoval *et al*., 2008), decreased Bnip3l abundance can result in an overall decrease in the number of mature erythrocytes despite a robust reticulocyte response. As observed in the current studies, 2-BE administration in mice results in extravascular erythrocyte destruction and splenomegally consistent with sustained downregulation of Bnip3l.

2-BE 7-day treatment induces genomic instability in the BM. A decrease in the expression of transcripts that contribute to mechanisms involved in genomic stability was supported in the BM in response to 2-BE treatment. These mechanisms include the predicted decreases in the transcriptional activity of Trp53 (p53) and Brca1 protein levels, which are supported by 57 and 47 gene expression changes, respectively (Supplementary Table 6 and data not shown). Trp53 and Brca1 have been shown to function in cell cycle

TABLE 4
Increased Spleen RNA Expression Changes ($p < 0.05$) of Nucleated Erythrocyte Markers after 7 Days of 2-BE Treatment

Gene symbol	Gene name	Fold change
Ache	Acetylcholinesterase	3.76
Slc4a1	Erythrocyte membrane protein band 3, Diego blood group	19.6
Cd47	CD47 antigen	2.12
Tfrc	Transferrin receptor	16.5
Gypa	Glycophorin A	11.4
Hbb-y	Hemoglobin Y, beta-like embryonic chain	2.18
Hbb-bh1	Hemoglobin Z, beta-like embryonic chain	1.56
Hba-x	Hemoglobin X, alpha-like embryonic chain in Hba complex	1.37
Rhd	Rh blood group, D antigen	9.82
Itga4	Integrin, alpha 4	1.36

checkpoint control and induce cell cycle arrest upon DNA damage (Bargonetti and Manfredi, 2002; Hartman and Ford, 2003). Therefore, decreased functionality of both proteins impairs the ability of the cell to compensate for and repair DNA damage secondary to increased cell proliferation resulting in decreased genomic stability.

DISCUSSION

The present study was aimed at gaining a better understanding of the molecular mechanisms underlying hemangiosarcoma formation to help determine the relevance of drug-induced hemangiosarcomas in mice to cancer risk in humans. As summarized in Figure 5, CNM on transcriptomic data from BM, spleen, and liver of mice treated with the hemangiosarcoma-causing agent, 2-BE, revealed multiple interrelated processes that comprise a mechanistic model of hemangiosarcoma formation. Specifically, analysis of the transcriptomic data demonstrated support for an inflammatory response in the liver, including activated macrophages and cytokine production in response to 2-BE. This response is consistent with previous reports investigating the mechanism of action of 2-BE (Corthals *et al.*, 2006; Klaunig and Kamendulis, 2005). Importantly, our data demonstrate the potential role for hypoxia, secondary to 2-BE–induced hemolysis, as an initiating event in hemangiosarcoma. In addition, CNM supported a role for Epo signaling that, coupled with decreased genomic stability in hematopoietic organs, could stimulate the proliferation of EPCs and increase the probability of spontaneous mutations of this cell type. These results also support the recruitment of proliferating EPCs in the BM to sites of inflammation in the liver as an additional contributor to hemangiosarcoma formation. This study illustrates the use of such a model to further the mechanistic understanding of hemangiosarcoma. Importantly, the mode of action outlined in Figure 5 is consistent with that published in a recent review, where a generalized mode of action of hemangiosarcoma formation was proposed (Cohen *et al.*, 2009).

Hypoxia Can Contribute to the Initiation of Hemangiosarcoma

2-BE–induced hypoxia in the liver, spleen, and BM was demonstrated by transcriptomics, CNM, and phenotypically via the use of Hypoxyprobe. We propose that hypoxia may mediate previously identified mechanisms of 2-BE–induced hemangiosarcoma. For example, hypoxia can serve as an initiating event to iron-induced oxidative stress previously observed in response to 2-BE treatment (Klaunig and Kamendulis, 2005; Nyska *et al.*, 2004). Local tissue hypoxia generates an acidic environment that stimulates iron release from hemosiderin leading to the production of hydroxyl radicals *in vitro* (Ozaki *et al.*, 1988), and without an acidic environment, iron is not as efficiently released from hemosiderin (Ozaki *et al.*, 1988). Furthermore, Hif1a, the hypoxia-responsive transcription factor, has been shown to induce ROS production, likely via the Fenton reaction (Hervouet *et al.*, 2008), which has also been implicated in the oxidative stress effects of 2-BE (Klaunig and Kamendulis, 2005). Therefore, it is possible that hypoxia may function upstream of and contribute to iron-induced oxidative stress in response to 2-BE.

In addition to its role in oxidative stress, hypoxia and activation of Hif1a have been shown to induce processes that can increase the supply of oxygen. This is achieved through the transcription of genes that function in processes such as angiogenesis and EC proliferation (Otrock *et al.*, 2009; Yamakawa *et al.*, 2003). Among these genes is Vegf, a well-known growth factor that has been shown to induce angiogenesis (Forsythe *et al.*, 1996; Levy *et al.*, 1995). Since hemangiosarcomas are EC-derived tumors (Mendenhall *et al.*, 2006), the discovery of high expression levels of Hif1a, Hif2a, as well as the Hif target genes, Vegf and Epo, in a renal angiosarcoma (Rathmell *et al.*, 2004) is consistent with the role of these factors in EC proliferation.

Continuous Epo Signaling Results in Erythropoiesis and EPC/EC Proliferation in Spleen and BM

As described above, the proposed mechanistic model for induction of hemangiosarcoma identifies continuous Epo signaling in the BM as a key event leading to the differentiation and proliferation of EPCs and ECs in hematopoietic organs (BM and spleen). The RBC hemolysis induced by 2-BE likely serves as the initial stimulus for Epo signaling (Leng *et al.*, 1999). The induction of Epo serves to ameliorate the anemia resulting from RBC hemolysis, by signaling for production of erythrocytes. Interestingly, the present study found transcriptomic data consistent with a decrease in Bnip3l (also called Nix) protein levels in the BM of 2-BE–treated mice compared to controls. Bnip3l is a Bcl2-interacting protein family member (Schweers *et al.*, 2007) that, when knocked

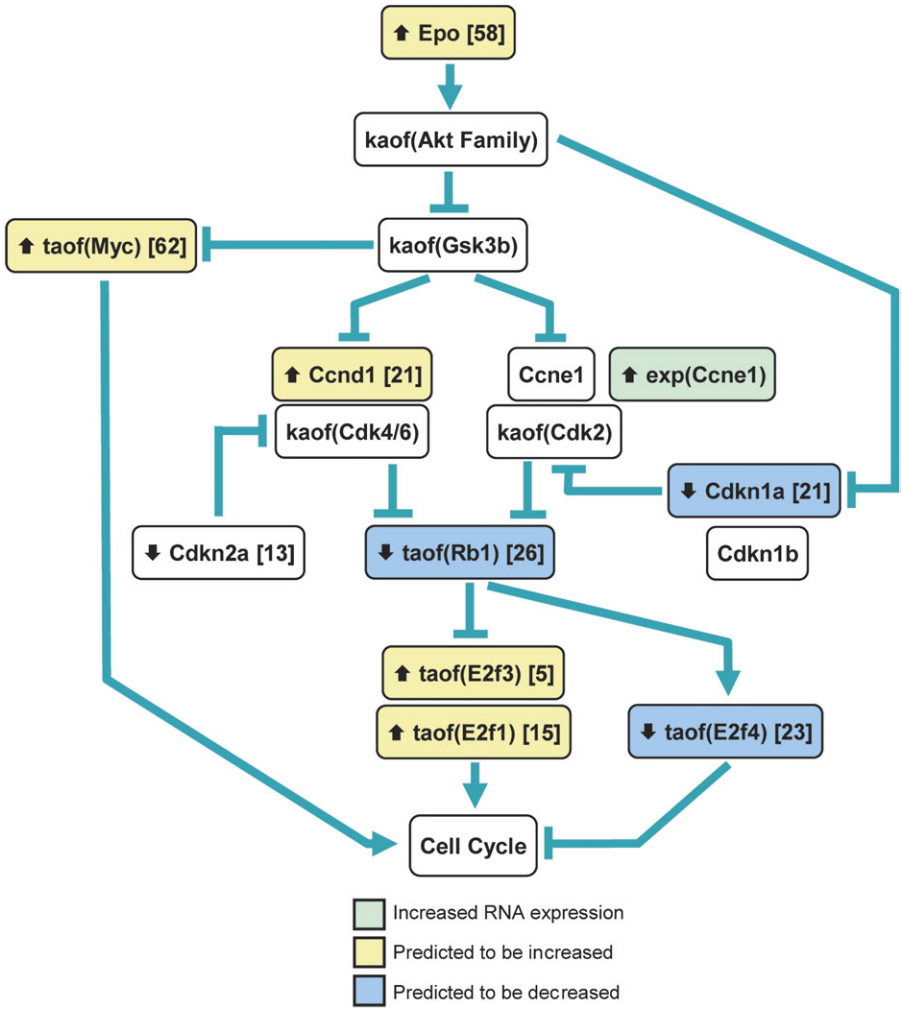

FIG. 4. Seven-day 2-BE treatment leads to cell cycle progression in the BM. CNM based on BM gene expression changes predicts increased Epo signaling that leads to changes in activity and abundance of proteins resulting in cell cycle progression. For notation and color guide, refer to Figures 1 and 3. Genes that support the hypotheses listed in this figure can be found in Supplementary Table 4.

down, has been shown to hinder the process of mitochondria removal and apoptosis in erythrocytes during their maturation (Diwan *et al*., 2007; Schweers *et al*., 2007; Sandoval *et al*., 2008). Loss of Bnip3l has also been characterized using Nix−/− mice, which demonstrate anemia, reduced erythrocyte lifespan *in vivo*, reticulocytosis, and splenomegaly (Diwan *et al*., 2007). Decreased Bnip3l protein levels in response to 2-BE, therefore, results in an increase in mitochondria-containing erythrocytes, which are targeted for removal by the spleen. Increased elimination of mature erythrocytes results in a sustained decrease in the number of mature erythrocytes despite robust reticulocytosis. This decrease in mature erythrocyes, in turn, leads to continuous Epo signaling in an attempt to replenish erythrocyte levels to normal values (Noguchi *et al*., 2008; Weidemann and Johnson, 2009). Reduced apoptosis of spleen and BM erythrocyte populations results in the aberrant survival of committed erythroblasts contributing to erythroblastosis (Diwan *et al*., 2007). Additionally, Bnip3l has been shown to be regulated by hypoxia, and deregulation has been associated with tumor growth (Zhang and Ney, 2009). Experimentally, downregulation of Bnip3l increased the growth of osteosarcoma cells in a tumor transplant model, suggesting that Bnip3l is needed to inhibit tumor growth under hypoxic conditions.

Epo has been shown in previous studies to stimulate EC and EPC proliferation (Bahlmann *et al*., 2003). EPCs derived from hematopoietic organs that circulate in the blood have the ability to differentiate into ECs (Shi *et al*., 1998). Sustained Epo signaling due to decreased Bnip3l levels and sustained effects on erythropoiesis would result therefore in continuous proliferation of ECs and EPCs, contributing to hemangiosarcoma formation. Supporting the notion of EPCs as central to hemangiosarcomas, EPC-like hematopoietic precursors have been shown to be the main source of ECs in canine hemangiosarcomas (Lamerato-Kozicki *et al*., 2006). Moreover, preliminary results have demonstrated that after 7-day treatment with 2-BE, there are increases in proliferation of

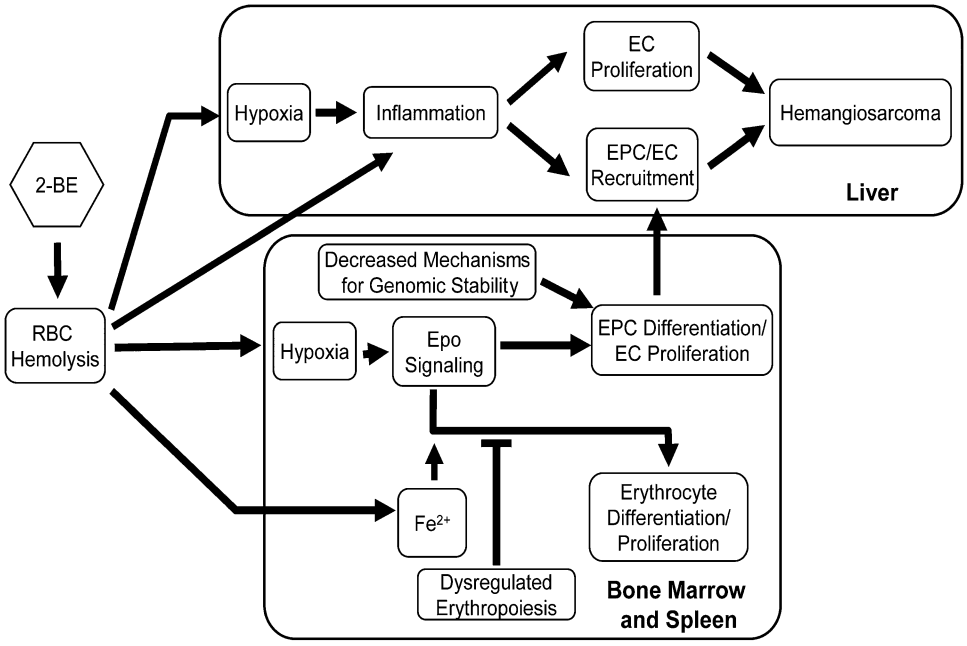

FIG. 5. Proposed mechanistic model of 2-BE–induced hemangiosarcoma. The proposed model is based on CNM analysis of transcriptomic data, EC proliferation, and Hypoxyprobe data from liver, spleen, and BM of mice treated for 4 h and 7 days with 2-BE. The main processes identified are (1) hypoxia, (2) dysregulated erythropoiesis, decreased genomic stability, and Epo signaling that can lead to EC proliferation and differentiation in the hematopoietic organs, and (3) inflammation that can lead to EC proliferation and EC/EPC recruitment in the liver.

ECs/EPCs in both spleen and BM (Criswell, K. A., Sokolowski, S., and Aubrecht, J.), consistent with the proposed mechanistic model.

Inflammation in the Liver Leads to Recruitment of EPCs/ECs from the Spleen and BM

The liver is the main site of hemangiosarcoma formation in mice in response to 2-BE. Therefore, processes identified in the liver define mechanisms that may preferentially lead to hemangiosarcoma formation in this organ. CNM of the liver gene expression data revealed activation of inflammatory processes after acute and chronic 2-BE treatment (Fig. 1). This response is consistent with previous 2-BE studies where activation of Kupffer cells and IL-6 induction were found (Corthals *et al*., 2006; NTP, 2000). These inflammatory processes can contribute to local hemangiosarcoma formation by recruiting circulating EPCs/ECs to the site of inflammation (Fan *et al*., 2008). Therefore, while EPC/ECs proliferate and acquire mutations secondary to increased cell proliferation in the BM and spleen, hemangiosarcomas are formed at the sites of recruitment of these EPC/ECs. Indeed, EPC/EC recruiting signals are commonly associated with sites of hemangiosarcoma formation. This has been observed for compounds such as *p*-nitroaniline and Elmiron, which induce hemangiosarcomas in the liver where iron accumulation and Kupffer cell activation is observed (Abdo *et al*., 2003; NTP, 1993, 2004). For other compound classes that induce mouse-specific hemangiosarcoma, such as peroxisome proliferator-activated receptor gamma agonists, pro-angiogenic growth factors have been observed (Sotiropoulos *et al*., 2006), and these may serve as EPC/EC recruiting signals (Chen *et al*., 2008). Taken together, these studies indicate a key role for EPC/EC recruiting signals in hemangiosarcoma formation, something that was also suggested in a recent review on hemangiosarcoma in rodents (Cohen *et al*., 2009).

Species-Specific Mechanisms Are Identified within the Mechanistic Model for Hemangiosarcoma

Hemangiosarcomas are rare in humans but are more commonly found in mice. Of the processes identified in this study, increased hypoxia exhibits species differences that may help explain the different rates of hemangiosarcoma occurrence between mice, rats, and humans. Because 2-BE causes hemolysis only in mice and rats, humans should not be subject to the subsequent hypoxia (Udden, 2002); therefore, the stimulus for sustained Epo signaling that results from 2-BE treatment does not occur in humans. Mice may also be more vulnerable to oxidative stress stemming from hypoxic conditions since they have been shown to have lower hepatic levels of the antioxidant, vitamin E, compared to rats and humans (Siesky *et al*., 2002). Thus, hypoxia as an initiating event to 2-BE–induced hemangiosarcoma is consistent with previously identified species-specific differences that predispose mice to hemangiosarcoma formation. Additionally, there are no reports of increased hemangiosarcomas in humans with chronic

hemolytic disease or in people living at high altitudes, so hypoxia alone is likely not an operational component of hemangiosarcoma formation in humans. Interestingly, Mori-Chavez *et al*. (1970) report that exposure of mice to high altitude does increase the incidence of spontaneous ovarian angiomas.

In summary, this is the first study to use transcriptomic data linked to pathways analysis to develop a mechanistic, temporal, and multiorgan model of hemangiosarcoma. The resulting model confirms that 2-BE induces macrophage activation and inflammation in the liver as previously proposed (Corthals *et al*., 2006; Klaunig and Kamendulis, 2005). In addition, the model specifically supports local tissue hypoxia, increased Epo signaling and erythropoiesis in the spleen and BM, and suppression of mechanisms that contribute to genomic stability as contributing factors to hemangiosarcoma in mice (Fig. 6). The key processes emerging from this model are sustained Epo signaling in the BM leading to proliferation of EPCs/ECs and recruitment signals for EPCs/ECs in the liver, the main site of hemangiosarcoma formation. Finally, these mechanisms, and in particular hypoxia as an initiating event, are consistent with a generalized mode of action framework that was developed with multiple other mouse-specific hemangiosarcoma-causing agents and that was published in a recent review (Cohen *et al*., 2009).

SUPPLEMENTARY DATA

Supplementary Figures 1–3, Tables 1–6, and other supplementary materials are available online at http://toxsci.oxfordjournals.org/.

ACKNOWLEDGMENTS

The authors gratefully acknowledge Martin Sanders, Chin-Hu Huang, and Damir Simic for their execution of the hypoxia studies; Marc Roy, Alan Opsahl, and Timothy Coskran for their expertise in generating and analyzing the Hypoxyprobe IHC data; and Susan Eddy for her help with BM isolations.

REFERENCES

Abdo, K. M., Johnson, J. D., and Nyska, A. (2003). Toxicity and carcinogenicity of Elmiron in F344/N rats and B6C3F1 mice following 2 years of gavage administration. *Arch. Toxicol.* **77,** 702–711.

Abdo, K. M., Murthy, A. S., Haseman, J. K., Dieter, M. P., Hildebrandt, P., and Huff, J. E. (1982). Carcinogenesis bioassay in rats and mice fed diets containing 2-biphenylamine hydrochloride. *Fundam. Appl. Toxicol.* **5,** 201–210.

Arteel, G. E., Raleigh, J. A., Bradford, B. U., and Thurman, R. G. (1996). Acute alcohol produces hypoxia directly in rat liver tissue in vivo: Role of Kupffer cells. *Am. J. Physiol.* **271,** 494–500.

Bahlmann, F. H., DeGroot, K., Duckert, T., Niemczyk, E., Bahlmann, E., Boehm, S. M., Haller, H., and Fliser, D. (2003). Endothelial progenitor cell proliferation and differentiation is regulated by erythropoietin. *Kidney Int.* **64,** 1648–1652.

Bahlmann, F. H., De Groot, K., Spandau, J. M., Landry, A. L., Hertel, B., Duckert, T., Boehm, S. M., Menne, J., Haller, H., and Fliser, D. (2004). Erythropoietin regulates endothelial progenitor cells. *Blood* **103,** 921–926.

Ballermann, B. J., Dardik, A., Eng, E., and Liu, A. (1998). Shear stress and the endothelium. *Kidney Int. Suppl.* **67,** S100–S108.

Bargonetti, J., and Manfredi, J. J. (2002). Multiple roles of the tumor suppressor p53. *Curr. Opin. Oncol.* **14,** 86–91.

Blander, G., Bhimavarapu, A., Mammone, T., Maes, D., Elliston, K., Reich, C., Matsui, M. S., Guarente, L., and Loureiro, J. J. (2009). SIRT1 promotes differentiation of normal human keratinocytes. *J. Invest. Dermatol.* **129,** 41–49.

Bouscary, D., Pene, F., Claessens, Y. E., Muller, O., Chrétien, S., Fontenay-Roupie, M., Gisselbrecht, S., Mayeux, P., and Lacombe, C. (2003). Critical role for PI 3-kinase in the control of erythropoietin-induced erythroid progenitor proliferation. *Blood* **101,** 3436–3443.

Bristow, R. G., and Hill, R. P. (2008). Hypoxia and metabolism. Hypoxia, DNA repair and genetic instability. *Nat. Rev. Cancer* **8,** 180–192.

Burgering, B. M., and Kops, G. J. (2002). Cell cycle and death control: Long live forkheads. *Trends Biochem. Sci.* **27,** 352–360.

Chambers, S. M., Boles, N. C., Lin, K. Y., Tierney, M. P., Bowman, T. V., Bradfute, S. B., Chen, A. J., Merchant, A. A., Sirin, O., and Weksberg, D. C. (2007). Hematopoietic fingerprints: An expression database of stem cells and their progeny. *Cell Stem Cell* **1,** 578–591.

Chan, P. (1993). NTP technical report on the toxicity studies of Riddelliine (CAS No. 23246-96-0) administered by gavage to F344 rats and B6C3F1 mice. *Toxic. Rep. Ser.* **27,** 1–D9.

Chen, L., Tredget, E. E., Wu, P. Y., and Wu, Y. (2008). Paracrine factors of mesenchymal stem cells recruit macrophages and endothelial lineage cells and enhance wound healing. *PLoS One* **3,** e1886.

Chow, L. M., and Baker, S. J. (2006). PTEN function in normal and neoplastic growth. *Cancer Lett.* **241,** 184–196.

Cohen, S. M., Storer, R. D., Criswell, K. A., Doerrer, N. G., Dellarco, V. L., Pegg, D., Wojcinski, Z., Malarkey, D. E., Jacobs, A. C., Klaunig, J. E., *et al.* (2009). Hemangiosarcoma in rodents: Mode-of-action evaluation and human relevance. *Toxicol. Sci.* **111,** 4–18.

Corthals, S. M., Kamendulis, L. M., and Klaunig, J. E. (2006). Mechanisms of 2-butoxyethanol-induced hemangiosarcomas. *Toxicol. Sci.* **92,** 378–386.

Ding, Y., Jiang, W., Su, Y., Zhou, H., and Zhang, Z. (2004). Expression and purification of recombinant cytoplasmic domain of human erythrocyte band 3 with hexahistidine tag or chitin-binding tag in Escherichia coli. *Protein Expr. Purif.* **34,** 167–175.

Diwan, A., Koesters, A. G., Odley, A. M., Pushkaran, S., Baines, C. P., Spike, B. T., Daria, D., Jegga, A. G., Geiger, H., and Aronow, B. J. (2007). Unrestrained erythroblast development in Nix−/− mice reveals a mechanism for apoptotic modulation of erythropoiesis. *Proc. Natl. Acad. Sci. U.S.A.* **104,** 6794–6799.

El-Hage, J. (2004). *Preclinical and Clinical Safety Assessments for PPAR Agonists,* Drug Information Association meeting, Washington, DC.

Elliott, B. M., and Ashby, J. (1997). Review of the genotoxicity of 2-butoxyethanol. *Mutat. Res.* **387,** 89–96.

Fan, Y., Ye, J., Shen, F., Zhu, Y., Yeghiazarians, Y., Zhu, W., Chen, Y., Lawton, M. T., Young, W. L., and Yang, G. Y. (2008). Interleukin-6 stimulates circulating blood-derived endothelial progenitor cell angiogenesis in vitro. *J. Cereb. Blood Flow Metab.* **28,** 90–98.

Forsythe, J. A., Jiang, B. H., Iyer, N. V., Agani, F., Leung, S. W., Koos, R. D., and Semenza, G. L. (1996). Activation of vascular endothelial growth factor gene transcription by hypoxia-inducible factor. *Mol. Cell Biol.* **16,** 4604–4613.

Gentleman, R. (2005). Bioinformatics and computational biology solutions using R and bioconductor. *Stat. Biol. Health* **xix,** 397–420.

Gentleman, R., Carey, V. J. C., Bates, D. M., Bolstad, B., Dettling, M., Dudoit, S., Ellis, B., Gautier, L., Ge, Y., and Gentry, J. (2004). Bioconductor: Open software development for computational biology and bioinformatics. *Genome Biol.* **5,** R80.

Ginouvès, A., Ilc, K., Macías, N., Pouysségur, J., and Berra, E. (2008). PHDs overactivation during chronic hypoxia "desensitizes" HIFalpha and protectscells from necrosis. *Proc. Natl. Acad. Sci. U.S.A.* **105,** 4745–50.

Goldberg, B., and Stern, A. (1977). The mechanism of oxidative hemolysis produced by phenylhydrazine. *Mol. Pharmacol.* **13,** 832–839.

Hartman, A. R., and Ford, J. M. (2003). BRCA1 and p53: Compensatory roles in DNA repair. *J. Mol. Med.* **81,** 700–707.

Heinemann, I. U., Jahn, M., and Jahn, D. (2008). The biochemistry of heme biosynthesis. *Arch. Biochem. Biophys.* **474,** 238–251.

Hervouet, E., Cizkova, A., Demont, J., Vojtísková, A., Pecina, P., Franssen-van Hal, N. L., Keijer, J., Simonnet, H., Ivánek, R., Kmoch, S., *et al.* (2008). HIF and reactive oxygen species regulate oxidative phosphorylation in cancer. *Carcinogenesis* **29,** 1528–1537.

Hiroyama, T., Miharada, K., Sudo, K., Danjo, I., Aoki, N., and Nakamura, Y. (2008). Establishment of mouse embryonic stem cell-derived erythroid progenitor cell lines able to produce functional red blood cells. *PLoS One* **3,** e1544.

Irizarry, R. A., B. H., Collin, F., Beazer-Barclay, Y. D., Antonellis, K. J., Scherf, U., and Speed, T. P. (2003). Exploration, normalization, and summaries of high density oligonucleotide array probe level data. *Biostatistics* **4,** 249–264.

Jelkmann, W. (2004). Molecular biology of erythropoietin. *Intern. Med.* **43,** 649–659.

Klaunig, J. E., and Kamendulis, L. M. (2005). Mode of action of butoxyethanol-induced mouse liver hemangiosarcomas and hepatocellular carcinomas. *Toxicol. Lett.* **156,** 107–115.

Lamerato-Kozicki, A. R., Helm, K. M., Jubala, C. M., Cutter, G. C., and Modiano, J. F. (2006). Canine hemangiosarcoma originates from hematopoietic precursors with potential for endothelial differentiation. *Exp. Hematol.* **34,** 870–878.

Leng, H. M., Albrecht, C. F., Kidson, S. H., and Folb, P. I. (1999). Erythropoietin production in anemia associated with experimental cancer. *Exp. Hematol.* **5,** 806–810.

Levy, A. P., Levy, N. S., Wegner, S., and Goldberg, M. A. (1995). Transcriptional regulation of the rat vascular endothelial growth factor gene by hypoxia. *J. Biol. Chem.* **270,** 13 333–13 340.

Mendenhall, W. M., Mendenhall, C. M., Werning, J. W., Reith, J. D., and Mendenhall, N. P. (2006). Cutaneous angiosarcoma. *Am. J. Clin. Oncol.* **29,** 524–528.

Mori-Chavez, P., Upton, A. C., Salazar, M. J., and Conklin, J. W. (1970). Influence of altitude on late effects of radiation in RF/Un mice: Observations on survival time, blood changes, body weight, and incidence of neoplasms. *Cancer Res.* **30,** 913–928.

Noguchi, C. T., Wang, L., Rogers, H. M., Teng, R., and Jia, Y. (2008). Survival and proliferative roles of erythropoietin beyond the erythroid lineage. *Expert Rev. Mol. Med.* **10,** e36.

NTP (1989). Toxicology and carcinogenesis studies of para-chloroaniline hydrochloride (CAS No. 20265-96-7) in F344/N rats and B6C3F1 mice (gavage studies). *Natl. Toxicol. Program Tech. Rep. Ser.* **351,** 1–256.

NTP (1993). Toxicology and carcinogenesis studies of p-nitroaniline (CAS No. 100-01-6) in B6C3F1 mice (gavage studies). *Natl. Toxicol. Program Tech. Rep. Ser.* **418,** 1–203.

NTP (1997). Toxicology and carcinogenesis studies of tetrafluoroethylene (CAS No. 116-14-3) in F344 rats and B6C3F1 mice (inhalation studies). *Natl. Toxicol. Program Tech. Rep. Ser.* **450,** 1–321.

NTP (2000). Toxicology and carcinogenesis studies 2-butoxyethanol (CAS NO. 111-76-2) in F344/N rats and B6C3F1 mice (inhalation studies). *Natl. Toxicol. Program Tech. Rep. Ser.* **484,** 1–290.

NTP (2004). Technical report on the toxicology and carcinogenesis studies of Elmiron (Cas No. 37319-17-8) in F344/N rats and B6C3F1 mice (gavage studies). *Natl. Toxicol. Program Tech. Rep. Ser.* 7–289.

Nyska, A., Haseman, J. K., Kohen, R., and Maronpot, R. R. (2004). Association of liver hemangiosarcoma and secondary iron overload in B6C3F1 mice—The National Toxicology Program experience. *Toxicol. Pathol.* **32,** 222–228.

O'Neill, L. A., and Bowie, A. G. (2007). The family of five: TIR-domain-containing adaptors in Toll-like receptor signalling. *Nat. Rev. Immunol.* **7,** 353–364.

Otrock, Z. K., Hatoum, H. A., Awada, A. H., Ishak, R. S., and Shamseddine, A. I. (2009). Hypoxia-inducible factor in cancer angiogenesis: Structure, regulation and clinical perspectives. *Crit. Rev. Oncol. Hematol.* **70,** 93–102.

Ozaki, M., Kawabata, T., and Awai, M. (1988). Iron release from haemosiderin and production of iron-catalysed hydroxyl radicals in vitro. *Biochem J.* **250,** 589–595.

Park, J., Kamendulis, L. M., and Klaunig, J. E. (2002a). Mechanisms of 2-butoxyethanol carcinogenicity: Studies on Syrian hamster embryo (SHE) cell transformation. *Toxicol. Sci.* **1,** 43–50.

Park, J., Kamendulis, L. M., and Klaunig, J. E. (2002b). Effects of 2-butoxyethanol on hepatic oxidative damage. *Toxicol. Lett.* **126**(1), 19–29.

Peters, L. L., Jindel, H. K., Gwynn, B., Korsgren, C., John, K. M., Lux, S. E., Mohandas, N., Cohen, C. M., Cho, M. R., Golan, D. E., *et al.* (1999). Mild spherocytosis and altered red cell ion transport in protein 4. 2-null mice. *J. Clin. Invest.* **103,** 1527–1537.

Pollard, J., Jr., Butte, A. J., Hoberman, S., Joshi, M., Levy, J., and Pappo, J. (2005). A computational model to define the molecular causes of type 2 diabetes mellitus. *Diabetes Technol. Ther.* **7,** 323–336.

R Development Core Team. (2007). *R: A Language and Environment for Statistical Computing*. R Foundation for Statistical Computing, Vienna, Austria. ISBN 3-900051-07-0. Available at: http://www.R-project.org. Accessed July 6, 2009.

Rathmell, W. K., Acs, G., Simon, M. C., and Vaughn, D. J. (2004). HIF transcription factor expression and induction of hypoxic response genes in a retroperitoneal angiosarcoma. *Anticancer Res.* **24,** 67–169.

Ruan, H., Hacohen, N., Golub, T. R., Van Parijs, L., and Lodish, H. F. (2002). Tumor necrosis factor-alpha suppresses adipocyte-specific genes and activates expression of preadipocyte genes in 3T3-L1 adipocytes: Nuclear factor-kappaB activation by TNF-alpha is obligatory. *Diabetes* **51,** 1319–1336.

Sandoval, H., Thiagarajan, P., Dasgupta, S. K., Schumacher, A., Prchal, J. T., Chen, M., and Wang, J. (2008). Essential role for Nix in autophagic maturation of erythroid cells. *Nature* **454,** 232–235.

Schweers, R. L., Zhang, J., Randall, M. S., Loyd, M. R., Li, W., Dorsey, F. C., Kundu, M., Opferman, J. T., Cleveland, J. L., and Miller, J. L. (2007). NIX is required for programmed mitochondrial clearance during reticulocyte maturation. *Proc. Natl. Acad. Sci. U.S.A.* **104,** 19500–19505.

Shi, Q., Rafii, S., Wu, M. H., Wijelath, E. S., Yu, C., Ishida, A., Fujita, Y., Kothari, S., Mohle, R., Sauvage, L. R., *et al.* (1998). Evidence for circulating bone marrow-derived endothelial cells. *Blood* **92,** 362–367.

Siesky, A. M., Kamendulis, L. M., and Klaunig, J. E. (2002). Hepatic effects of 2-butoxyethanol in rodents. *Toxicol. Sci.* **70,** 252–260.

Smyth, G. K. (2004). Linear models and empirical Bayes methods for assessing differential expression in microarray experiments. *Stat. Appl. Genetics Mol. Biol.* **3,** 1.

Sotiropoulos, K. B., Clermont, A., Yasuda, Y., Rask-Madsen, C., Mastumoto, M., Takahashi, J., Della Vecchia, K., Kondo, T., Aiello, L. P., and King, G. L. (2006). Adipose-specific effect of rosiglitazone on vascular permeability and protein kinase C activation: Novel mechanism for PPARgamma agonist's effects on edema and weight gain. *FASEB J* **20,** 1203–1205.

Stroka, D. M., Burkhardt, T., Desbaillets, I., *et al*. (2001). HIF-1 is expressed in normoxic tissue and displays an organ-specific regulation under systemic hypoxia. *FASEB J* **15,** 2445–2453.

Tao, D., Shen, Y., Feng, X., and Chen, H. (2000). The application of CD71 and Hoechst33258 to staining method for sorting fetal nucleated red blood cells in the peripheral blood of pregnant women. *Zhonghua Yi Xue Yi Chuan Xue Za Zhi* **17,** 352–354.

Toth, B., Nagel, D., Patil, K., Erickson, J., and Antonson, K. (1978). Tumor induction with the N'-acetyl derivative of 4-hydroxymethyl-phenylhydrazine, a metabolite of agaritine of Agaricus bisporus. *Cancer Res*. **38,** 177–180.

Udden, M. M. (2002). In vitro sub-hemolytic effects of butoxyacetic acid on human and rat erythrocytes. *Toxicol. Sci*. **69,** 258–264.

Urao, N., Okigaki, M., Yamada, H., Aadachi, Y., Matsuno, K., Matsui, A., Matsunaga, S., Tateishi, K., Nomura, T., Takahashi, T., *et al*. (2006). Erythropoietin-mobilized endothelial progenitors enhance reendothelialization *via* Akt-endothelial nitric oxide synthase activation and prevent neointimal hyperplasia. *Circ. Res*. **98,** 1405–1413.

Wagner, E. F., and Risau, W. (1994). Oncogenes in the study of endothelial cell growth and differentiation. *Semin. Cancer Biol*. **5,** 137–145.

Weidemann, A., and Johnson, R. S. (2009). Nonrenal regulation of EPO synthesis. *Kidney Int*. **75,** 682–688.

Yamakawa, M., Liu, L. X., Date, T., Belanger, A. J., Vincent, K. A., Akita, G. Y., Kuriyama, T., Cheng, S. H., Gregory, R. J., and Jiang, C. (2003). Hypoxia-inducible factor-1 mediates activation of cultured vascular endothelial cells by inducing multiple angiogenic factors. *Circ. Res*. **93,** 664–673.

Yi, Z., Cohen-Barak, O., Hagiwara, N., Kingsley, P. D., Fuchs, D. A., Erickson, D. T., Epner, E. M., Palis, J., and Brilliant, M. H. (2006). Sox6 directly silences epsilon globin expression in definitive erythropoiesis. *PLoS Genet*. **2,** e14.

Zhang, J., and Lodish, H. F. (2005). Identification of K-ras as the major regulator for cytokine-dependent Akt activation in erythroid progenitors in vivo. *Proc. Natl. Acad. Sci. U.S.A*. **102,** 14605–14610.

Zhang, J., and Ney, P.a (2009). Role of Bnip3l and Nix in cell death, autophagy, and mitophagy. *Cell Death Differ*. **16,** 934–946.